DEVELOPMENT OF LOW CONTENT PHOSPHOGYPSUM WASTE COMPOSITES MODIFIED BY LIME-FLY ASH-BASIC OXYGEN FURNACE SLAG

T.P. MASHIFANA[1, 2 *] , F.N. OKONTA[2], F. NTULI[1]

[1]*University of Johannesburg, Department of Chemical Engineering, P.O. Box 17011, Doornfontein 2088, South Africa. Tel.:+27 11 559 6527, Email: tmashifana@uj.ac.za (Corresponding author)*

[2]*University of Johannesburg, Department of Civil Engineering Sciences, P.O. Box 524, Auckland Park 2000, South Africa.*

The generation and disposal of phosphogypsum (PG) is a worldwide challenge, due to the environmental pollution posed by the material. The contaminants laden in the material are the major limitations for the utilisation of PG. Other materials considered as wastes such as fly ash (FA) and basic oxygen furnace slag (BOF slag) are generated by numerous industrial activities and disposed into environment. This study investigated the use of three wastes materials for the development of a composite applicable for road construction. Two types of PG were investigated, namely citric acid treated PG (TPG), for the removal of the contaminants and raw PG (RPG). Lower content PG containing 20% and 30% were investigated and modified with FA, Lime (L) and BOF slag. The effect of particle size distribution (PSD) on unconfined compressive strength development, durability of the composites and hydration products contributing to strength development were studied. Modification of PG with FA-L-BOF slag significantly improved the unconfined compressive strength of PG. The PG content of 20% for the RPG and TPG yielded the highest strengths of 7.4 MPa and 5.4 MPa, respectively when cure at elevated temperatures. Normal curing of the composites over 7 days and 28 also showed an increase in strength development. Particle size played a significant role in the unconfined compressive strength development. Kieserite, calcium aluminium sulphate and calcite were the predominant hydration products formed during the curing process.

Keywords: *Phosphogypsum, environment, hydration, fly ash, slag*

1. Introduction

Residual deposits of Phosphogypsum are readily available in large quantities in South Africa and currently are landfilled or pumped into the sea, as there are limitations to engineering applications due to the radionuclides content [1]. Phosphogypsum (PG), fly ash (FA) and basic oxygen furnace slag (BOF slag) are normally discharged to the environment without any treatment resulting to contamination of the environment, occupation of large areas of land and pollution of soil and ground water [2]. According to the available documented data an estimated 100-300 million tons of PG is generated worldwide per annum [3-5]. In the year 2014/15 approximately 119,2-million tons of coal was consumed, which generated approximately 34,4-million tons (28,9%) of fly ash in South Africa [6]. Only 7% of the Eskom fly ash is sold from six of the 13 Eskom coal-fired power stations, as compared to 50 to 60% in other countries [6].

In respect to PG, a minimal amount of about 15% PG is utilized other applications such as agricultural purposes and in building and road construction due to the presence of radionuclides [7-12], which limits its applications. The use of industrial wastes of phosphogypsum and fly ash as potential stabilizer of marginal construction materials has been reported by Mashifana et.al. [13]. Yang et.al. previously conducted a study on making building materials from calcined phosphogypsum. The study was focused on autoclaved PG and its use in making load-bearing wall bricks [14]. Autoclaved PG was prepared from original waste PG with steam pre-treatment. The crystalline phase, morphology, and thermal characteristics of original waste PG and autoclaved PG were investigated by XRD, SEM, and SDT. Then bricks of the size of Chinese standard brick (230 mm x114 mm x 65 mm) were prepared from different types of PG in the PG-fly ash–lime–sand system. The results obtained revealed that the compressive strength of bricks from autoclaved PG by lower-pressure steam at 0.12 MPa, 120^{o}C for 16 hours was much higher. The flexural strength and compressive strength of the bricks reached 4.0 MPa and 15.0 MPa respectively. Previous studies have been carried out to use phosphogypsum in preparing building materials, such as blocks, bricks and plasters [15-18], of which non-fired bricks has become a significant research topic. At present, there are two kinds of processes to prepare non-fired bricks from phosphogypsum. One is the autoclaving curing process in which the green non-fired bricks are pressed at normal pressures (20–40 MPa) [19-20]. The other one is the autoclave cured at the pressure of 0.8–1.2 MPa and the temperature of 100–180^{o}C for 4–8 h, as investigated by Altun and Sert [8]. However, Zhou et.al. [21], does not totally agree with Altun and Sert [8] to use autoclaved phosphogypsum to

* Autor corespondent/*Corresponding author*,
E-mail: tmashifana@uj.ac.za

produce building material. According to Zhou et.al. [21], they identified some gaps in the process; the major drawback of this process is the exorbitant energy consumption in the course of autoclave-curing. The other is the high-pressure press-forming process, in which the non-fired bricks are press-formed at a very high pressure of about 80 MPa and air-dried at ambient conditions [22-26]. The key shortfalls of this process are the need of using high-pressure forming equipment and the low compressive strength of the prepared brick products (generally less than 10 MPa).

In the study by Zhou et al. [21] to utilize waste phosphogypsum to prepare non-fired bricks by the novel Hydration Recrystallization process, the press-formed green bricks were hot-dried at 180°C to dihydrate gypsum ($CaSO_4.2H_2O$) into semi hydrated gypsum ($CaSO_4.0.5H_2O$), and then water-immersed to in situ recrystallize gypsum ($CaSO_4.2H_2O$) crystals, and finally air-dried naturally to obtain the non-fired brick products [21]. A series of the experiments were conducted according to this process, and results showed that the optimal composite composed of 75.0% phosphogypsum, 19.5 % river sand, 4.0% Portland cement and 1.5% hydrated lime, and the corresponding compressive strength, water-saturated compressive strength and bending strength of the as-prepared bricks were 21.8 MPa, 13.7 MPa and 5.2 MPa, respectively.

A solution to find ways to use wastes in building and road construction is of great interest. In this study the three readily available wastes material were used to develop composites that can be utilised for building and construction applications. Waste PG was modified with lime, waste FA and BOF slag. The resulting composite unconfined compressive strength meets a minimum of 3.5 MPa according to South African standards TRH 14 [27] and is suitable for application in road construction elements.

2. Experimental procedure

2.1. Composites preparation

The PG treated with citric acid for 24 hours was thoroughly washed with water, until only clear water was discharging from the bottom of the filter press. TPG was then dried in the oven at 80°C for 24 hours. This final product was further used in the study. The RPG and TPG content of 20% and 30% were investigated in matrix containing fly ash-lime and BOF slag. The content of BOF slag was kept constant at 10% in all the mix designs. The following proportions as presented in Table 1 were investigated.

2.2. Casting, curing, determination of unconfined compressive strength and pH

The Maximum dry density and Optimum moisture content at different RPG and TPG content were determined and the results obtained are presented in Table 2. Three specimens per test were then cast in a 100 mm×100 mm×100 mm moulds. The three cast specimens per test were cured for 96 hours at an elevated temperature of 80°C. After the curing process the unconfined compressive strength of the specimens was determined by following the ASTM method D698. [28], using the strength measuring machine with a loading rate of 15 kN/min. The results presented are an average of three casts. The specimens for the RPG and TPG were casted and cured at ambient temperature. The strength was allowed to develop over 7 days and 28 days. After the curing period the unconfined compressive strength was determined. To determine the pH of PG, a pH meter was used to measure the PG/water mixture, prepared by adding 50 g of PG into 100 ml of deionized water under continuous stirring and measuring the pH after 30 minutes. An average of three samples is presented in the results.

Table 1
Composite of RPG and TPG

Material	PG%	Lime:Fly ash 1:2 (%)	BOF slag %
RPG	20	1:2 (70)	10
RPG	30	1:2 (60)	10
TPG	20	1:2 (70)	10
TPG	30	1:2 (60)	10

Table 2
Maximum dry density and Optimum moisture content of RPG and TPG

	RPG 20	RPG30	TPG 20	TPG 30
MDD (kgm^{-3})	1120	1131	1080	1110
OMC (%)	22	24	23	20

The RPG and TPG composites after curing are shown in Figure 1. The cubes were solid and could be handled without any breakage or crumbling indicating good workability of the material.

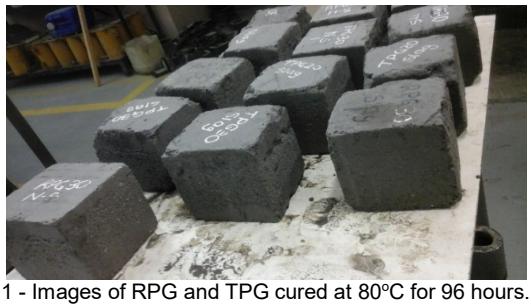

Fig.1 - Images of RPG and TPG cured at 80°C for 96 hours.

2.3. Characterization

The oxidic composition of the materials utilized was studied by X-Ray Flourescence (XRF-Rigaku ZSX Primus II) and the mineralogy with X-Ray Diffraction (XRD- Rigaku Ultima IV).The solid particles morphology was captured by using a Scanning Electron Microscope (SEM, model Tecson Vega 3 XMU). A Malvern Masterizer 2000 particle size analyser was used to study the

Table 3

Oxidic composition of the raw material

Component (%)	Raw PG	L	FA	Treated PG	BOF slag
F	1.063				
Al_2O_3	0.227	0.279	28.00	0.091	4.67
SiO_2	1.370	0.503	47.90	0.857	14.12
P_2O_5	1.283	0.0288	0.725	0.719	1.21
SO_3	51.01	0.191	0.606	54.40	
CaO	43.65	73.40	5.130	42.75	43.81
TiO_2			2.470		0.27
Fe_2O_3	0.1214	0.225	4.830	0.048	0.27
MgO					3.53
MnO					2.84
Total Radionuclides	0.6198			0.405	

particle size distribution (PSD) of the material used.

2.3.1. Oxidic composition

The oxidic composition of the material used is presented in Table 3.

The predominant oxides in RPG was calcium oxide and sulphur trioxide and some radionuclides. Treatment of PG reduced the radionuclides that may result into hindering strength development. TPG was mainly laden with sulphur trioxide and calcium oxide. Calcium oxide was predominant in the hydrated lime used. Fly ash consisted of constituent such as Silica, calcium oxide, ferrous iron and titanium oxide were the major constituents in fly ash. For BOF slag, calcium oxide relative proportion is was the highest followed by that of silica and aluminium.

2.3.2.Morphology of the raw material

Morphology of raw material are shown in Figure 2.

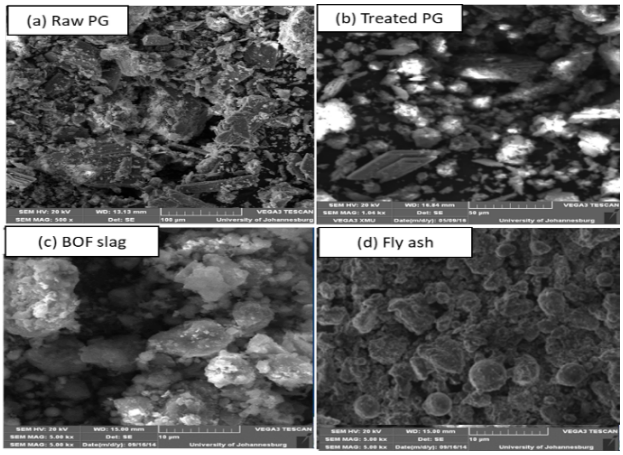

Fig.2 – Morphology of the raw material (a) RPG (b) TPG (c) BOF slag and (d) Fly ash.

A smooth surface is observed for the raw PG composites and unlike the treated PG surface which looks bristly. The scanning electron microscope image of BOF slag shows that the material mainly consists of larger sub rounded to angular particles with the surface having a rough surface texture. BOF slag larger particles increased the contact between the particles cementing the particles together and increasing the unconfined compressive strength. Spherical structured particles which are irregular shaped and cenospheres are visible in the fly ash material. The irregular shaped flakes represent carbon that is unburnt and normally visible as granular, lamellar, flat and intermediate particles [29].

2.3.3.Particle size distribution (determination of the moments)

The PSD data was transformed into its moments using equation 1 and 2. The number density function was calculated from the volume based histogram $vol\%$ versus L_i where i indicates the size sub-range and the particle concentration ($vol\%$) were generated by laser diffraction and the volume shape factor k_v equal to $\pi/6$ was used [30].

$$n(L)dL = \sum_i \frac{vol\%_i \times conc(vol\%)}{100} \cdot \frac{1}{k_v L^{-3}} \quad (1)$$

$$m_j = \int_0^\infty L^j n(L)dL \quad (2)$$

The first four moments (0^{th}, 1^{st}, 2^{nd} and 3^{rd}) are of special interest and are related to the total number, length, area and volume of solid per unit volume of suspension respectively [30].

2.4. Durability (24 hours soak test)

Three specimens at different PG contents and different water content (at OMC values presented in Table 2) for both RPG and TPG were cast and cured for 96 hours, at a temperature of 80°C, following ASTM D559-03 [31]. After 96 hours the specimen were allowed to cool down and the weight determined. The specimens were soaked in a water bath for 24 hours, thereafter removed, any excess water on the surface of the specimen was wiped off and the specimens were weighed. The unconfined compressive strength was then determined. The porosity of the composites was determined by following ASTM C37-14a [32]. The composites were cured at the optimum temperature for 96 hours. The dry weight was determined and the composites soaked in water for 24 hours. After the soaking period the

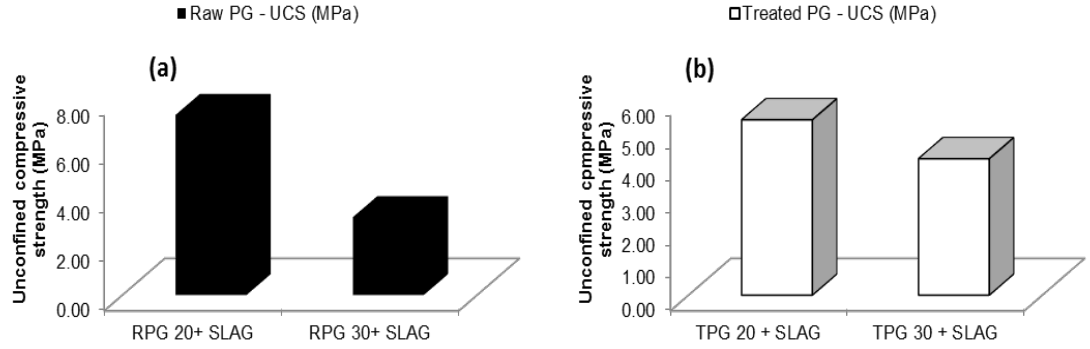

Fig.3 - (a) Unconfined compressive strength of (a) RPG cured at elevated temperature (b) TPG cured at elevated temperature.

wet composite were weighed. Open porosity was then calculated using equation 3.

$$f = \left(W_s - W_d / V\alpha \right) \quad (3)$$

Where *f* is open porosity, W_s is the mass of the soaked composite, W_d the mass of the dry composite, V the volume of the composite and α is the density of water.

2.5. Lime consumption calculation

A solution of ammonium acetate was prepared by dissolving 1.6 g of ammonium acetate into 100 ml of ethanol. A phenolphthalein solution of 0.2 ml was then added per every 100 ml of ethanol glycerol solvent in the ratio of 2:1. A finely ground, 1 g composite sample was added to 60 ml of the ethanol-glycerol and 2 g of anhydrous strontium nitrate added in a flask. The flask was connected to a condenser and the mixture boiled for 20 min. After 20 min the heater was switched off and the hot mixture was filtered. The filtrate was brought to boiling point and immediately titrated against the standard ammonium acetate solution to a colourless end point. The percent free lime was calculated following equation 4

$$\%\text{Free CH} = EVx100 \quad (4)$$

where *E* is the lime equivalent of the ammonium acetate solution (g/ml) and *V* is the volume of ammonium acetate titrated.

3.Results and discussions

3.1. Unconfined compressive strength

The unconfined compressive strength of low content RPG and TPG are presented in Figure 3(a) and Figure 3(b).

Figure 3(a) shows the unconfined compressive strength obtained when 20% and 30% raw PG was stabilised with lime, fly ash and basic oxygen furnace slag. The results show strengths of up to 7.4 MPa for the composite containing 20% PG and 4 MPa for the material with 30% PG. Increasing the PG content drastically reduced the unconfined compressive strength of the material by almost 50%. The material based on the resulting strength meets a minimum of 3.5 MPa making it suitable for application in road construction material.

Stabilization of 20% and 30% TPG yielded unconfined compressive strength of 5.4 MPa and 4.2 MPa, respectively, Figure 3(b). An increase in the PG content resulted into 28% reduction in the strength. The stabilised material with unconfined compressive strength of 5.4 and 4.2 MPa is classified as C2 material according to South African standards TRH 14, 1985 [27].The lowest PG content of 20% yielded the highest strength in both the RPG and TPG composites. TPG 30 proved to produce better strengths as compared to the RPG30 material. In respect to unconfined compressive strength and the voluminous utilization of PG, the treated PG would be the best material. It is very evident that phosphogypsum hastened the reaction between lime and fly ash. The study conducted by Shen et.al. [26], shows the highest strengths obtained with fly ash-lime-phosphogypsum being at PG content of 18-23%, and results similar to the findings in this study.

3.2. XRD analysis of the raw material and RPG and TPG

From Figures 4(a), the XRD patterns of the BOF slag samples have several overlapping peaks resulting from the numerous minerals present in the samples. Other researchers have reported similar, complex XRD patterns for BOF slag [33, 34]. The phases in fly ash are presented in Figure 4(b). Figures 4 (c) show that the predominant peak in hydrated lime was that of CH (2θ= 34.2°) with the intensity of 1400. Figure 4(d) shows the spectrum for the raw PG. A well-defined, highly crystalline material is associated with the diffraction peak of gypsum ($CaSO_4 \cdot 2H_2O$). Figure 4(e) show a predominant phase being that of Gypsum ($CaSO_4 \cdot 2H_2O$). Calcium aluminum sulphate from fly ash, lime and gypsum, quartz and kieserite ($MgSO_4 \cdot H_2O$) were some of the minerals detected. Treated PG material consisted mainly of gypsum (Figure 4(f)). Traces of coesite (SiO_2) and fayalite (Fe_2SiO_4) were also present. For TPG20 in Figure 4(g) Gypsum ($CaSO_4 \cdot 2H_2O$)

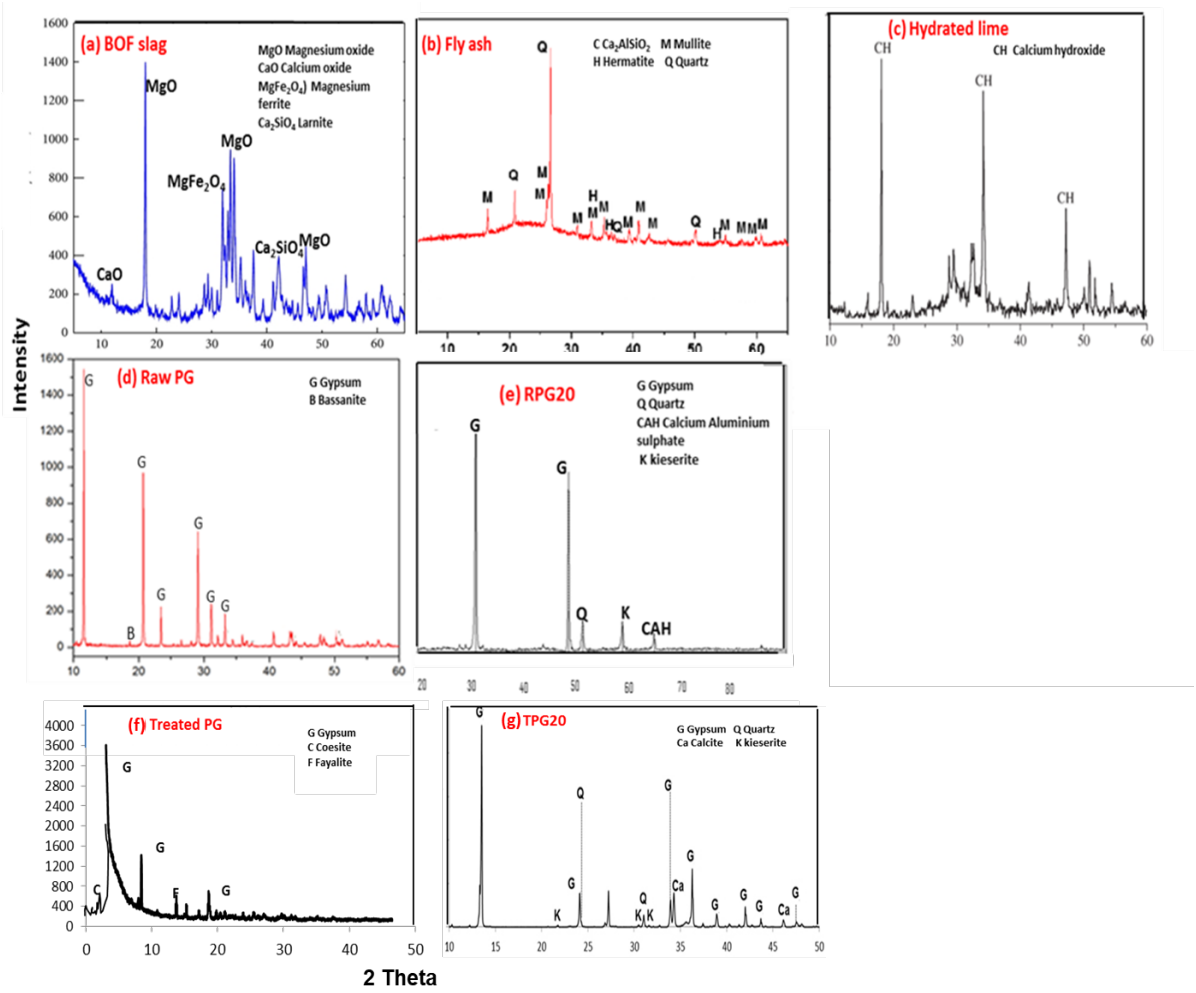

Fig.4 - XRD (a) BOF slag, (b) Fly ash, (c) Hydrated lime, (d) Raw PG, (e) RPG20 (f) Treated PG, (g) TPG20.

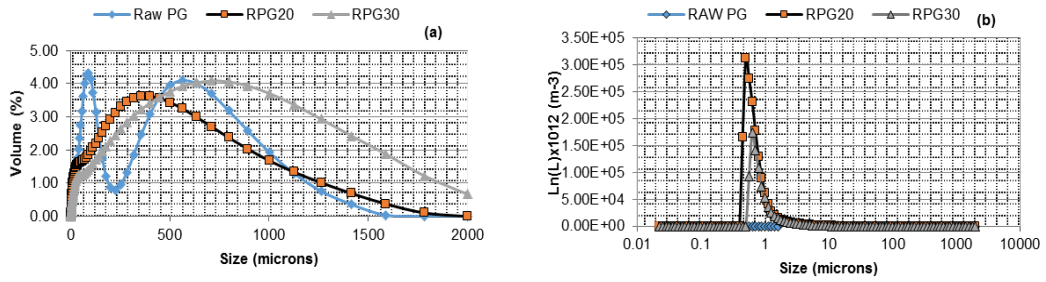

Fig.5 - (a) Volume distribution of raw PG and RPG composites (b) Number distribution of Raw PG and the RPG composites .

with XRD peaks at 13.45°, 23.91°, and 33.91° (2θ) was the most abundant phase. Magnesium sulphate ($MgSO_4 \cdot H_2O$) with XRD peaks at 30.44°, 31.13°, and 21.54° (2θ) and quartz (SiO_2) with peaks at 30.9 and 24.29° (2θ) were also detected. In RPG20 composite, kieserite ($MgSO_4.H_2O$) and calcium aluminium sulphate ($Ca_6Al_2(SO_4)_3(OH)_{12} \cdot 26H_2O$) were the predominant hydration products formed. Calcite and Kieserite were the predominant new hydration products formed during the curing process in TPG20 composite. Kieserite is one of the common mineral in both RPG20 and TPG20 indicating that it also played a significant role in the high strengths obtained in these composites.

3.3. Particle size distribution (PSD)

Figures 5(a) and 5(b) show the volume distribution and the number distribution of the raw RPG and RPG composites respectively.

The raw PG had a bimodal volume distribution with a significant change to a unimodal distribution for RPG20 and RPG30, Figure 5(a). The median changed from 709 µm to 360 µm for the RPG20 and to 1002 µm for RPG30. There was a modal shift to the left in the number distribution from that of the RPG compared to its respective composites, indicating a generation of fines, Figure 5(b). The increase in area under the curve for the composites was visible indicating an increase in the particles number for both RPG20 and RPG30,

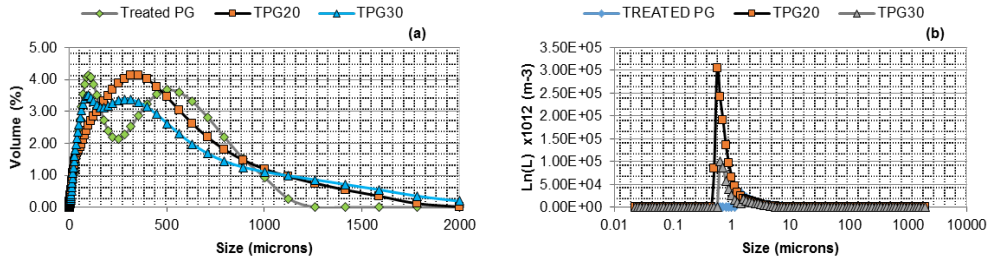

Fig.6 - (a) Volume distribution between treated PG and TPG composites (b) Number distribution of TPG and the TPG composites.

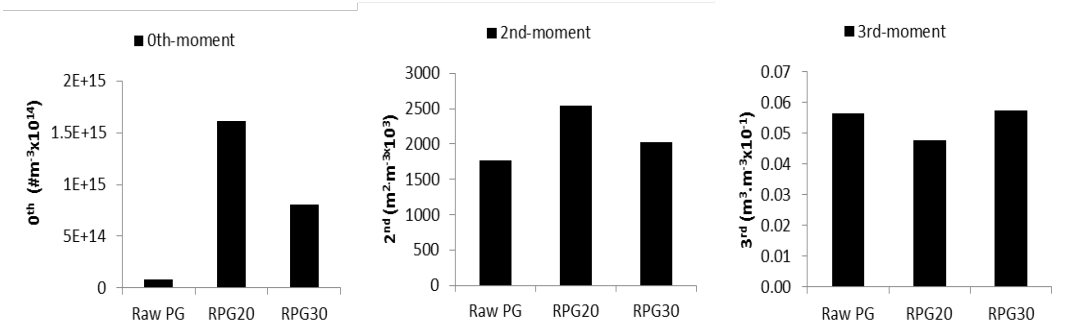

Fig.7 - Moments of PSD: 0th- particle number, 2nd- surface area, 3rd –volume of particle for RPG.

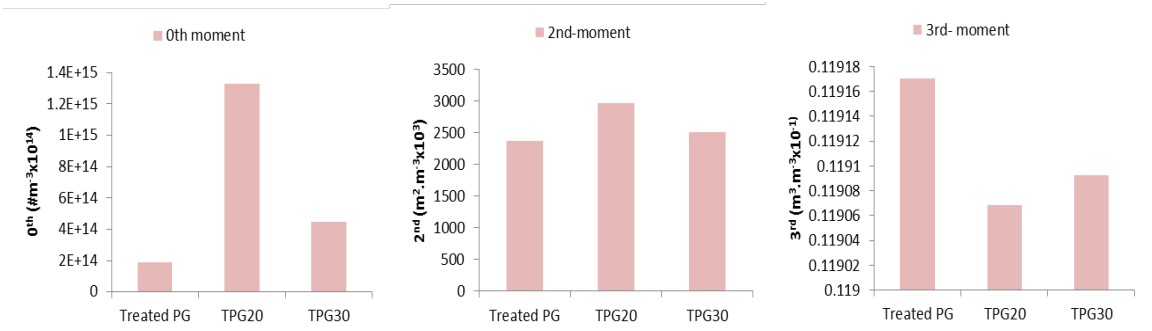

Fig.8 - Moments of Particle size distribution: 0th- particle number, 2nd- surface area, 3rd volume of particles for TPG.

with RPG20 having the highest number of finer particles.

Figures 6(a) and 6(b) show the volume distribution and number distribution of the treated PG and the TPG composites respectively.

TPG20 composite had a unimodal volume distribution, whereas TPG30 composite had a bimodal distribution volume distribution similar to that of TPG, Figure 6(a). A bimodal distribution might result from a process involving breakup of larger particles or multiple sources of particles. There was a median change from 632 µm to 399 µm for TPG20 and to 447 µm for TPG30. The number distribution showed a significant modal size shift to the left indicating that there were more fine particles generated in TPG composite samples, Figure 6(b).

3.4. Moments of PSD

The moments of the PSD for RPG and TPG is presented in Figure 7 and Figure 8, respectively.

The results presented in Figure 7 show that there was a significant increase in the particle number from RPG to RPG20 and RPG30 composites, with RPG20 having the highest number of particles. This might be a result of particle breakage from larger to finer particles. An increase in surface area is also evident from the RPG to the composites, showing that particle breakage to smaller particles resulted in an increase in exposed external particle surface area. No significant change in the volume of particles was observed indicating insignificant particle size enlargement by growth of the composite particles.

There was an increase in the particle number and the surface area for the composite samples TPG20 and TPG30 as compared to TPG as illustrated in Figure 8 volume of particles for the TPG and the composites were between 0.11907 and 0.11916 $m^3.m^{-3}x10^{-1}$, showing that there was no significant change in particle size as a result of particles growth. The fines generated in both RPG and TPG composites show that during the curing of the composites there was particle breakage from larger particles to smaller and finer particles. Chen et.al [35] conducted a study investigating the effects of particle size on mechanical properties of a TiC containing tool steel by hot isostatic press and reported that fine particles are more effective in filling pores and prevent crack propagation

resulting in high unconfined compressive strength. This mechanism might have played a role in the high unconfined compressive strengths obtained for RPG20 and TPG20 composites.

3.5. pH of RPG and TPG

The RPG and TPG composites pH is shown in Figure 9.

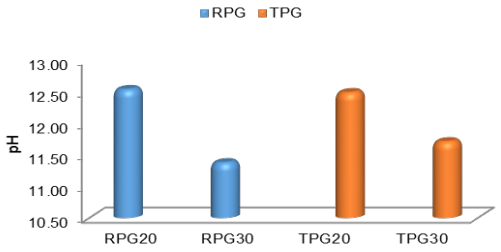

Fig.9 - pH of RPG and TPG composites

The lower PG content of 20% showed the highest pH for both RPG and TPG, at 12.54 and 12.49, respectively. This shows that the composites with higher pH resulted in the higher unconfined compressive strength, indicating that higher pH promoted the pozzolanic reaction which contributed to strength development.

3.6. Lime consumption

The lime consumption results for the RPG and TPG composites is presented in Table 4.

Table 4

Lime consumption

Composite	RPG20	RPG30	TPG20	TPG30
Lime consumption	84%	59%	87%	63%

The lowest PG content of 20 yielded the highest lime consumption as compared to the PG

30 composites for both RPG and TPG. The content of lime:fly ash was the highest in PG20 at 70% and only 60% in PG30 composite, therefore there was more lime in PG20 than PG30. In PG20 there is a higher content of silica and lime available for hydration reaction. This is evident from the higher unconfined compressive strength obtained in the lower PG content composites. The results obtained agree to those of Wang who reported that an increase in lime consumption is due to the availability of lime for the hydration reaction [36].

3.7. Durability (soaking)

Table 5 shows the unconfined compressive strength variation after the composites were soaked in water for 48 hours.

Table 5

Unconfined compressive strength of RPG and TPG after 24 hours soaking

	RPG20	RPG30	TPG20	TPG30
UCS before soaking	7.4	4.0	5.4	4.2
UCS after 24 hours soaking (MPa)	6.5	3.1	4.9	4.1

Soaking RPG20, RPG30, TPG20, TPG30 composites for 24 hours resulted in strength reduction of 13.84%, 29.03 %, 10.20% and 2.38%, respectively. RPG30 had the highest strength loss in all the composites. TPG30 proved to have the least strength loss as compared to the composite containing 20% PG. The unconfined compressive strength obtained shows that in respect to

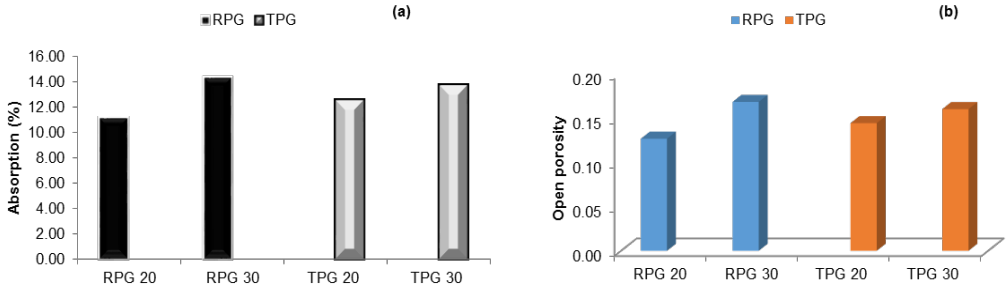

Fig.10 - (a) Water absorption of RPG and TPG composites (b) Open porosity of RPG and TPG composites

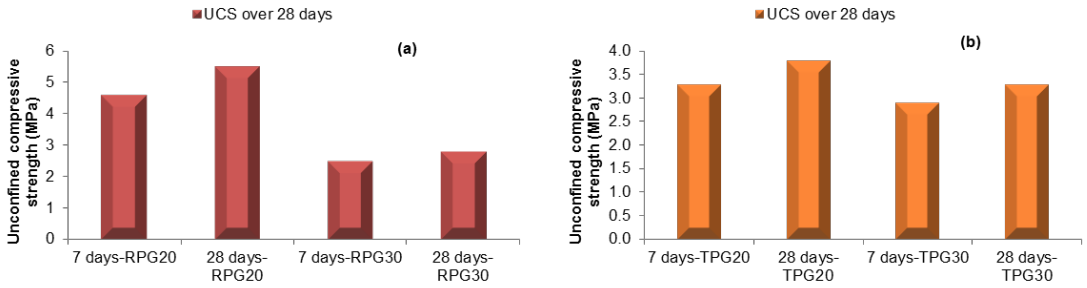

Fig.11 - Unconfined compressive strength development of (a) RPG over 28 days (b) TPG over 28 days

strength, the 20% PG material meets the minimum requirements of a structural clay load bearing non exposed masonry of ASTM C34-13 [37].

The composites water absorption after soaking in water for 24 hours and the porosity of the composites are shown in Figure 10(a) and Figure 10(b), respectively.

The RPG30 composite proved to be the composite with highest water absorption and this is the composite that yielded the least strength after 24 hours soaking. RPG20 had the lowest water absorption of 11.23%, followed by TPG20 with 12.6%, Figure 10(a). This shows that RPG20 and TPG20 composites had low water uptake associated with low material porosity, as indicated in Figure 10(b).

3.8. Strength development of RPG and TPG

The strength development over 28 days for the RPG and TPG is shown in Figure 11 (a) and Figure 11 (b).

Figure 11(a) depicts the RPG20 and RPG30 strength development for 7 days and 28 days. From the results, it is evident that there was an increase in unconfined compressive strength from 7 to 28 days in both the composites for all the mix designs. The strength development in RPG20 is higher than that of RPG30 over 28 days, showing that the rate of strength development was faster in the RPG20 as compared to RPG30. The results presented in Figure 11(b) shows that over 28 days there was an increase in the unconfined compressive of TPG20 and TPG30. The rate of strength development was the fastest in the TPG20 composite. Comparing the obtained strengths to the composites cured at elevated temperatures over 96 hours, there is a significant difference in the strength. This shows that temperature had an impact on the strength development of the composites. In curing under normal temperatures there is less energy for hydration to occur, therefore making the strength development process to be slow. This is evidenced by lower strength for normal curing at 7 and 28 days.

3.9. The effect of Basic Oxygen Furnace Slag on the strength development

Table 6 shows the unconfined compressive strength before and after the BOF slag was added into the composite mix design.

Table 6
Unconfined compressive strength of RPG and TPG without BOF slag.

	RPG20	RPG30	TPG20	TPG30
UCS without BOF slag (MPa)	4.8	2.9	2.3	1.2
UCS with BOF slag (MPa)	7.4	4.0	5.4	4.2

Introduction of BOF slag had a positive impact on the unconfined compressive strength of the composites. The strength for all the composite showed an increment after the stabilisation with BOF slag. The strength improvement of over 100 % is observed for both TPG20 and TPG30. BOF is a well-known aggregate in civil engineering for building and road construction and it proved to be a suitable material/activator to stabilize both the raw and treated PG and improve the unconfined compressive strength.

4. Conclusion

In this study the three readily available wastes material, waste phosphogypsum (PG) modified with lime (L), waste fly ash (FA) and waste of basic oxygen furnace slag (BOF slag) were used to develop composites that can be used for building and construction applications. The resulting composite unconfined compressive strength meets a minimum of 3.5 MPa according to South African Standard TRH 14/1985, and is suitable for application in road construction elements.

The best results concerning mechanical strengths were by using untreated (RPG) and treated (TPG) phosphogypsum, in a proportion of 20%. Composite materials obtained through the use of phosphogypsum, at a rate of 20%, were recorded mechanical strength (UCS) of 7.4 MPa, fulfilling conditions for use as road building materials.

It is found that, the unconfined compressive strength (UCS) of composite materials obtained with 20% phosphogypsum (PG20), is influenced by the particle size distribution (PSD), the pH content of composite, the content of basic oxygen furnace slag (BOF slag) and the sample storage temperature (maturing).

The fines generated in both RPG and TPG composites show that during the curing of the composites there was particle breakage from larger to smaller and finer particles.

The composites that yielded highest unconfined compressive strength are that which exhibited highest pH for both untreated (RPG20) and treated (TPG20).

Modification of untreated and treated phosphogypsum with basic oxygen furnace slag resulted into 100% strength improvement in all the mix designs (RPG20, RPG30, TPG20 and TPG30).

Longer curing periods of up to 28 days resulted into unconfined strength development for all the mix designs and highest strengths obtained for untreated (RPG20) and treated (PG20) phosphogypsum.

In studying lime consumption for untreated (RPG) and treated (TPG) phosphogypsum, both the materials with 20% phosphogypsum (PG20) resulted into higher lime consumption of 84% and 87%, respectively.

Untreated and treated composites with

30% phosphogypsum (PG30) proved to be more porous as compared to the composites wit 20% phosphogypsum (PG20) and absorbed more water.

Acknowledgement

The authors would like to thank the University of Johannesburg, National Research Foundation of South Africa for the financial support and iThemba laboratory for the analysis.

REFERENCES

1. T.P. Mashifana, F.N. Okonta, F. Ntuli, Geotechnical properties and application of lime modified phosphogypsum waste, Materials Science (MEDŽIAGOTYRA), 2018, **24**(3), 312.
2. W. Hou, X. Chen, G. Song, Q. Wang and C.C, Chang, Effects of copper and cadmium on heavy metal polluted waterbody restoration by duckweed (Lemna minor). Plant physiology and biochemistry, 2007, **45**(1), 6.
3. N. Willey, Environmental Plant Physiology, Gerland Science, 2015
4. H. Tayibi, A. López-Delgado, M. Choura, C. Gascó, N. Navarro, F.J. Alguacil and F.A. López Gómez, Preliminary studies of a phosphogypsum stabilisation process using a sulphur polymer matrix, 2009.
5. Y.P. Yang, The method of manufacturing the high-strength building bricks of phosphogypsum. State Intellectual Property Office of the People's Republic of China, 2007.
6. M. Rycroft, Exploring the many uses of fly ash, EE Publishers, 2017.
7. X. Msila, F. Labuschagne, W. Barnard and D. G. Billing, Radioactive nuclides in phosphogypsum from the lowveld region of South Africa. South African Journal of Science, 2016, **112**, 1.
8. I.A. Altun, Y. Sert, Utilization of weathered phosphogypsum as set retarder in Portland cement. Cement and Concrete Research, 2004, **34**(4), 677.
9. M. Haschke, B. Friedrich, S. Stopic, D. Panias, P. Schneider, C. Dittrich, Extraction of critical technology elements and radionuclides from phosphogypsum tailings. Opportunities in Processing of Metal Resources, 2016.
10. E. Saadaoui, N. Ghazel, C. Romdhane, N. Massoudi, Phosphogypsum: potential uses and problems–a review. International Journal of Environmental Studies, 2017, **74**(4), 558.
11. N. Willey, N., 2015, Environmental Plant Physiology, Gerland Science, 2016.
12. Q. Chen, Q. Zhang, A. Fourie, C. Xin, Utilization of phosphogypsum and phosphate tailings for cemented paste backfill. Journal of environmental management, 2017, **201**, 19.
13. T.P. Mashifana, F.N. Okonta, F. Ntuli, Geotechnical properties and micro structure of lime-fly ash-phosphogypsum stabilised soil. Advances in Civil Engineering, 2018, 1.
14. J. Yang, W. Liu, L. Zhang and B. Xiao, Preparation of load-bearing building materials from autoclaved phosphogypsum. Construction and Building Materials, 2009, **23**(2), 687.
15. L. Ma, P. Ning, S. Zheng, X. Niu, W. Zhang and Y. Du, Reaction mechanism and kinetic analysis of the decomposition of phosphogypsum via a solid-state reaction. Industrial & Engineering Chemistry Research, 2010, **49**(8), 3597.
16. S. Kumar, A perspective study on fly ash–lime–gypsum bricks and hollow blocks for low cost housing development. Construction and Building Materials, 2002, **16**(8), 519.
17. J. Zhou, D. Yu, Z. Shu, T. Li, Y. Chen and Y. Wang, A novel Two-step Hydration Process of preparing cement-free non-fired bricks from waste phosphogypsum. Construction and Building Materials, 2014, **73**, 222.
18. M. Singh, Effect of phosphatic and fluoride impurities of phosphogypsum on the properties of selenite plaster. Cement and Concrete Research, 2003, **33**(9), 1363.
19. J.P. Xia, S.S. Zhang and X. Wang, The method of preparing non-fired bricks by the phosphogypsum cement materials to solidify the phosphorus slag. State Intellectual Property Office of the People's Republic of China, 2009.
20. X.L. Yin, The method of manufacturing the high strength and proof-water and proof-fire non-fired bricks of the industrial by-production phosphogypsum. State Intellectual Property Office of the People's Republic of China, 2007.
21. J. Zhou, H. Gao, Z. Shu, Y. Wang and C. Yan, Utilization of waste phosphogypsum to prepare non-fired bricks by a novel Hydration–Recrystallization process. Construction and Building Materials, 2012**,** **34**, 114.
22. Z.W. Chen, The method of manufacturing the non-fired bricks of phosphogypsum. State Intellectual Property Office of the People's Republic of China, 2008.
23. Z.J. Li, T. Shen and Q. Xie, The method of manufacturing the environmental and high-pressure non-fired bricks of phosphogypsum. State Intellectual Property Office of the People's Republic of China, 2005.
24. Y.P. Yang, The method of manufacturing the high-strength building bricks of phosphogypsum. State Intellectual Property Office of the People's Republic of China, 2007.
25. T.B. Zhang and J.H. Chi, The method of producing the non-fired bricks of phosphogypsum. State Intellectual Property Office of the People's Republic of China, 2000.
26. W. Shen, M. Zhou and Q. Zhao, Study on lime–fly ash–phosphogypsum binder. Construction and Building Materials, 2007, **21**(7), 1480.
27. Technical Recommendations for Highways 14, Guidelines for Road Construction Materials, 1985.
28. ASTM, Standard Test Methods for Laboratory Compaction Characteristics of Soil Using Standard Effort (12 400 ft-lbf/ft^3 (600 kN-m/m^3)). D698-07, 2012.
29. C.G. Vassileva, S.V. Vassilev, Methods for Characterization of Composition of Fly Ashes from Coal-Fired Power Stations: A critical overview. Energy and Fuels, 2005, **19**, 1084.
30. F. Ntuli and A.E. Lewis, Kinetic modelling of nickel powder precipitation by high-pressure hydrogen reduction. Chemical Engineering Science, 2009, **64**(9), 2202.
31. ASTM, Standard Test Methods for Wetting and Drying Compacted Soil-Cement Mixtures. D559-03, 2012.
32. ASTM, Standard Test Method for Water Absorption, Bulk Density, Apparent Porosity, and Apparent Specific Gravity of Fired Whiteware Products, Ceramic Tiles, and Glass Tiles. C373 - 14a, 2014.
33. M. Tossavainen,F. Engstrom, Q. Yang, N. Menad, M.L. Larsson and B. Bjorkman, Characteristics of steel slag under different cooling conditions, Waste management, 2007, **27**(10), 1335.
34. M. Nicolae, I. Vîlciu and F. Zaman, X-ray diffraction analysis of steel slag and blast furnace slag viewing their use for road construction. UPB Sci. Bull, 2007, **69**(2), 99.
35. J.K. Chen, T.P. Tang, S.F. Chan and S.H. Chang, Effects of Particle Size on Mechanical Properties of a TiC Containing Tool Steel by Hot Isostatic Press. Materials Transactions, 2008, **49**(3), 624.
36. S. Wang, Quantitative kinetics of pozzolanic reactions in coal/coal fired biomass fly ashes and calcium hydroxide (CH) mortars. Construction and Building Materials, 2014, **51**, 364.
37. ASTM, Standard Specification for Structural Clay Load-Bearing Wall Tile. C34-13, 2013

****